

# Supporting Information

Sebastián et al. 10.1073/pnas.1108220109

## SI Materials and Methods

**Animal Care, Generation of Animal Models, and Diet Treatments.** All animal work was performed in compliance with guidelines established by the University of Barcelona Committee on Animal Care. Mitofusin 2 (*Mfn2*)<sup>loxP/loxP</sup> mice were provided by David Chan (Division of Biology and Howard Hughes Medical Institute, California Institute of Technology, Pasadena, CA) (*Mfn2*<sup>tm3Dcc/Mmcd</sup>) (1) through Mutant Mouse Regional Resource Center. Homozygous *Mfn2*<sup>loxP/loxP</sup> mice were crossed either with a mouse strain expressing Cre recombinase under the control of promoter from MEF2C (*mef2C-73K-Cre*) (2) or with a mouse strain expressing Cre recombinase specifically in liver during neonatal life under the control of albumin promoter (*Alb-Cre*) (The Jackson Laboratory). Control and KO mice were littermates. Mice were kept under a 12-h dark/light cycle and were provided standard chow diet and water ad libitum. Male 10-wk-old mice were fed a standard diet or a high-fat diet (HFD) for 20 wk (10% or 60% calories from fat, D12451 and D12492; Research Diets). At the times indicated in the figure legends, mice were anesthetized with isoflurane and killed by cervical dislocation. Tissues used for RNA purification, protein extraction, or histology were prepared as published (3, 4).

**In Vivo Metabolic Measurements and Insulin Signaling Studies.** Serum samples were taken between 10:00 AM and 12:00 PM after an overnight fast or at the same time in fed conditions. Blood glucose was assayed with an Accu-Chek glucose monitor (Roche Diagnostics). Plasma was immediately separated by centrifugation at 4 °C and stored at –80 °C until assay. A glucose tolerance test (GTT) was performed on mice fasted for 16 h overnight. Glucose was measured at time 0, followed by i.p. injection of 2 g/kg glucose. Blood glucose levels were also measured at 5, 15, 30, 60, 90, and 120 min after injection. Plasma insulin levels were measured at 0, 15, 30, and 60 min after injection. An insulin tolerance test was performed on mice fasted for 4 h. Glucose was measured at time 0, followed by an i.p. injection of 0.75 U/kg insulin (Humalog). Blood glucose concentrations were measured at 15, 30, 45, 60, and 90 min after injection. Plasma insulin was determined with the Ultra Sensitive Mouse Insulin ELISA Kit (Crystal Chem).

To monitor in vivo insulin signaling in liver, mice were anesthetized with pentobarbital sodium (50 mg/kg) and injected with insulin (5 U/kg in 200  $\mu$ L) or an identical volume of PBS through the portal vein. Livers were removed 5 min later and immediately frozen in liquid nitrogen. In vivo insulin signaling in muscle was monitored by an i.p. injection of 5 U/kg of insulin, and soleus and gastrocnemius muscles were collected 15 min later. For ex vivo insulin signaling studies, soleus muscles were removed from anesthetized mice and incubated for 30 min in pre-gassed (95% O<sub>2</sub>, 5% CO<sub>2</sub>) Krebs–Ringer bicarbonate Hepes (KRBH) buffer plus 5 mM glucose at 37 °C and incubated for 15 min with or without 100 nM insulin in the same buffer. Soleus muscles were then frozen in liquid nitrogen. Tissues were homogenized in a buffer containing 50 mM Tris-HCl (pH 7.4), 150 mM NaCl, 1 mM EDTA, 1% Triton X-100, 2 mM sodium orthovanadate, 50 mM NaF, 20 mM sodium pyrophosphate, and the protease inhibitor mixture tablet (Roche). Lysates were used for immunoprecipitation and Western blot assays.

**Glucose Turnover Studies.** The mice were fasted for 6 h before the infusions. The mice were connected to the infusion apparatus at 2 h before the start of the infusions with free access to water. The

whole-body glucose utilization rate was determined under euglycemic-hyperinsulinemic conditions. Under physiological hyperinsulinemic conditions, insulin was infused at a rate of 4 mU/kg-min for 3 h, and D-[<sup>3</sup>H]3-glucose was infused at a rate of 30  $\mu$ Ci/kg-min. Throughout the infusion, blood glucose was assessed from blood samples (3.5  $\mu$ L) collected from the tip of the tail vein with a blood glucose meter when needed. Euglycemia was maintained by periodically adjusting a variable infusion of 10% or 16.5% glucose. Plasma glucose concentrations and D-[<sup>3</sup>H]3-glucose specific activity were determined in 5  $\mu$ L of blood sampled from the tip of the tail vein every 10 min during the last hour of the infusion as reported (5).

**Administration of Tauroursodeoxycholic Acid (TUDCA) or N-Acetylcysteine (NAC) in Mice.** TUDCA (Calbiochem) administration was carried out as described by Ozcan et al. (6). Briefly, control or L-KO 8-wk-old mice under normal chow diet were injected i.p. with 100  $\mu$ L of TUDCA or 100  $\mu$ L of PBS. TUDCA was administered twice a day in two divided doses (250 mg/kg at 6:30 AM and 6:30 PM, total 500 mg/kg per day). Control mice received the same volume of vehicle by i.p. injection at same time points. Treatment with the antioxidant NAC was performed on 8-wk-old mice (1% NAC in the drinking water).

**In Vivo Gene Transfer.** For electro-transfer studies, phosphorylated (p)CMV-microRNA (miRNA) or pDsRed2-Mito (Clontech) vectors were purified with a plasmid kit (EndoFree; Qiagen) and dissolved in 0.9% NaCl. Ten-week-old mice (C57BL6/J; Harlan) were used for pCMV-miRNA vector expression and 24-wk-old mice were used for pDsRed2-Mito vector expression. Mice were anesthetized with ketamine/xylazine, and, at 1 h before electro-transfer, muscles were pretreated with hyaluronidase (10 U per muscle) (7, 8). Afterward, naked plasmids were injected into the tibialis anterior and gastrocnemius muscles of both hindlimbs. We established that the optimal amount of plasmid to inject to achieve acceptable/satisfactory protein expression was 60  $\mu$ g and 100  $\mu$ g DNA in the former and latter, respectively. Ten pulses of 20 ms each were applied to each hindlimb at 175 V/cm and 1 Hz using an electroporator (ECM 830; BTX). The control animals were subjected to the same procedure after injection of saline and an empty vector. Experiments were performed at 2 wk after the electro-transfer for pCMV-truncated *Mfn2* and pCMV-miRNA vectors and 8 d after electro-transfer for pDsRed2-Mito vector.

**Cell Cultures and Adenoviral Transduction.** L6E9 or C2C12 cells were used in this study. Myoblasts were grown and allowed to differentiate into myotubes as previously described (9, 10). At day 3 of differentiation, myotubes were infected for 30 h at a multiplicity of infection (moi) of 100 pfu per cell, and all of the experiments were performed at 48 h after infection. L6E9 myotubes were treated with DMSO or the JNK inhibitor SP600125 (Calbiochem) for 16 h.

The following adenoviruses were used in this study: Ad-miRCt (encoding for a control miRNA) and Ad-miR2 (encoding for 5 miRNAs against *Mfn2*). miRNAs were generated with the Bock-it Pol II system from Invitrogen using the expression vector pcDNA 6.2 Gw/EmGFP/miR, which allows the cloning of several miRNAs in tandem and contains a GFP expression cassette. miRNAs were cloned by recombination into the pAdeno-CMV-V5 adenoviral vector (Invitrogen) by using the Gateway system. Adenoviruses were generated by transfection of the adenoviral expression vectors in a human embryonic kidney cell line (HEK

293). The adenoviruses generated were then amplified in HEK 293 cells, titrated with the Adeno-X Rapid Titer kit (Clontech), and used directly for cell transduction.

**Respiration Studies in Permeabilized Muscle, Isolated Liver Mitochondria, or Cultured Muscle Cells.** The respiration of permeabilized muscle fibers and liver mitochondria were measured at 37 °C by high-resolution respirometry with the Oxygraph-2k (Oroboros Instruments) as described (11). Mice were anesthetized with ketamine/xylazine, and the tibialis muscle was removed and placed on a plastic Petri dish containing 1 mL of ice-cold isolation solution [10 mM Ca-EGTA buffer (2.77 mM of CaK<sub>2</sub>EGTA + 7.23 mM of K<sub>2</sub>EGTA), 20 mM imidazole, 20 mM taurine, 50 mM K-Mes, 3 mM K<sub>2</sub>HPO<sub>4</sub>, 6.5 mM MgCl<sub>2</sub>, 5.7 mM ATP, 15 mM phosphocreatine, and 0.5 mM DTT (pH 7.1)]. Individual fiber bundles were separated with two pairs of sharp forceps and then permeabilized for 30 min in 2 mL of ice-cold isolation solution containing 50 µg/mL saponin. After rinsing muscle bundles in respiration medium [0.5 mM EGTA, 3 mM MgCl<sub>2</sub>·6H<sub>2</sub>O, 20 mM taurine, 10 mM KH<sub>2</sub>PO<sub>4</sub>, 20 mM Hepes, 1 g/L BSA, 60 mM K-lactobionate, and 110 mM sucrose (pH 7.1)], we weighed and transferred them (typically 2–4 mg wet weight) into the Oxygraph chamber containing 2 mL of air-saturated respiration medium. Isolated mitochondria were obtained as previously described (12). We used 500 µg of isolated mitochondria per chamber.

For permeabilized muscle fibers and liver isolated mitochondria, all respiration measurements were made in triplicate and followed this protocol: resting respiration (state 2, absence of adenylates) was assessed by the addition of 10 mM glutamate and 2 mM malate as the complex I substrate supply and then state 3 respiration was assessed by the addition of 2.5 mM ADP. The integrity of the outer mitochondrial membrane was established by the addition of 10 µM cytochrome c; no stimulation of respiration was observed. The addition of 10 mM succinate provided state 3 respiration with parallel electron input to complexes I and II. We examined ADP control of coupled respiration and uncoupling control through the addition of the protonophore carbonylcyanide-4-(trifluoromethoxy)-phenylhydrazone (FCCP) (optimum concentration for maximal flux). The addition of 0.5 µM rotenone resulted in inhibition of complex I, thereby allowing examination of O<sub>2</sub> flux with complex II substrate alone, whereas 2.5 µM antimycin A was added to inhibit complex III to observe nonmitochondrial respiration. The concentrations of substrates and inhibitors used were based on prior experiments conducted for optimization of the titration protocols.

Respirometry of cultured muscle cells was performed with the Seahorse Bioscience XF 24 platform.

**Measurement of H<sub>2</sub>O<sub>2</sub>.** H<sub>2</sub>O<sub>2</sub> levels in muscle cells or tissue extracts (liver and skeletal muscle) were measured with the Amplex Red hydrogen peroxide assay kit (Invitrogen) following the instructions of the manufacturer. Extracts were obtained in lysis buffer [50 mM Tris (pH 7.5), 150 mM NaCl, 1% Triton X-100, and 2 mM EDTA] and 50–100 µg of extract were used for the assay.

**Glucose Oxidation in the Incubated Muscle.** Mice were anesthetized with ketamine/xylazine, and the soleus muscle was carefully dissected and placed in 1 mL of cold KRBH buffer (pH 7.4), supplemented with 5 mmol/L glucose, until all of the muscles had been collected. Muscles were preincubated for 30 min at 37 °C in 2 mL of KRBH buffer containing 2% BSA (fatty acid free-BSA; Sigma) and 5 mmol/L glucose (incubation medium). The medium was gassed continuously with 95% O<sub>2</sub>, 5% CO<sub>2</sub>. The medium was then removed and replaced by 2 mL of fresh incubation medium containing 1 µCi/mL D-[U]-<sup>14</sup>C-glucose (Amersham Biosciences). The muscles were incubated for 60 min at 37 °C. Gassing was terminated after an initial 15 min. The test tubes were hermetically sealed with turnover flange rubber stoppers (Saint-Gobain

Verneret) with a center well that contained a piece of filter paper saturated with 200 µL of 1 M KOH. At the end of the incubation, the medium was acidified with 0.3 mL of 0.25 M H<sub>2</sub>SO<sub>4</sub> and gaseous <sup>14</sup>CO<sub>2</sub> released after the acidification was trapped in the filter paper. The vials were incubated at 37 °C for 60 min, and the filter papers were removed and transferred to vials for liquid scintillation counting.

**Histological Sample Preparation and Analysis.** For immunofluorescence assays, gastrocnemius muscles from control and Mfn2 KO mice were dissected, immersed in O.C.T. solution (Tissue-Tek), immediately frozen in liquid nitrogen-cooled isopentane (Sigma), and stored at –80 °C. Serial 10-µm sections of muscle samples were cut in a cryostat at –18 °C in the transversal plane. Tissues were collected onto room temperature 0.5% gelatin-coated glass slides. Briefly, sections were fixed in cold acetone for 20 min and air-dried for 30 min. After blocking in 10% FBS in PBS for 30 min, slides were incubated with mouse monoclonal Mfn2 antibody (Abcam) diluted 1/250 in blocking solution for 1 h followed by three 10-min washes in PBS. The samples were further incubated in donkey anti-mouse Alexa-Fluor 568-conjugated secondary antibodies (Invitrogen) for 1 h, followed by three 10-min washes in PBS. Hoechst 33342 (1/2,000; Molecular Probes) was used to label DNA. Sections were kept in the dark after secondary antibody incubation. Slides were finally covered with Fluoromount-G (Electron Microscopy Sciences) and let to dry overnight before being stored at 4 °C. Immunofluorescence microscopy of tissue was performed with a Leica TCS SP2 confocal scanning microscope adapted to an inverted Leica DMI 6000CS microscope to the acquisition of multiple tissular staining. Samples were scanned with a 20× Leitz objective and a zoom ranging from 1 to 3.5 using the LCS software from Leica. The fluorochromes used (Hoechst 33342 and Alexa-Fluor 568) were excited with the 405-nm (UV) and 568-nm laser lines, respectively. To avoid bleed-through effects (i.e., cross-talk of different fluorescence emission) in double-staining experiments, each dye was scanned independently. The projection format was 1024 × 1024 pixels. Images were acquired from six to eight optical sections. Figures were assembled from the TIF files by using National Institute of Mental Health's open software ImageJ.

**DNA and RNA Extraction and Real-Time PCR.** Mice were killed by cervical dislocation, and tissues were immediately frozen for RNA or DNA isolation. RNA from tissues was extracted by using a protocol combining TRIzol reagent (Invitrogen) and RNeasy Mini Kit columns (Qiagen) following the manufacturer's instructions. RNA was reverse-transcribed with the SuperScriptIII reverse transcriptase kit (Invitrogen). PCRs were performed with the ABI Prism 7900 HT real-time PCR machine (Applied Biosystems) and the SYBR Green PCR Master Mix or the TaqMan Probes 20× (Applied Biosystems). All measurements were normalized to β-actin and GAPDH. The oligonucleotide sequences for the primer pairs used were as follows (given as 5'- to -3'): phosphoenolpyruvate carboxykinase (PEPCK), forward: GTGCTGG-AGTGGATGTTCCGG, reverse: CTGGCTGATTCTGTTC-AGG; glucose 6-phosphatase, forward: TCCTGGGACAGAC-ACAAG, reverse: CAACTTTAATATACGCTATTGG; pyruvate carboxylase, forward: CTAGGTGCTTGCTGGTACAA; reverse: TCCAGACGCCGACATTT; and peroxisome proliferator-activated receptor γ coactivator 1α (PGC-1α), forward: GGAGCCG-TGACCACTGACA, reverse: TGGTTTGCTGCATGGTTCTG. Total DNA from tissues was extracted with the DNeasy Blood and Tissue Kit (Qiagen) following the manufacturer's recommendations. We quantified mitochondrial DNA by real-time PCR. Total DNA was used as a template and was amplified with specific oligodeoxynucleotides for mitochondrial DNA or Sdha (nuclear gene). The primers to amplify cytochrome c oxidase subunit II (Cox II) in mitochondrial DNA were as follows (given as 5'- to

-3'): forward, CTACAAGACGCCACAT and reverse, GAGAG-GGGAGAGCAAT. Other primers used to amplify mouse mitochondrial DNA in positions 1212 and 1352 were: forward, ACCGCAAGGGAAAGATGAAAG and reverse, AGGTAGCTC-GTTTGGTTTCGG. The primers to amplify nuclear DNA (mSDHA) were: forward, TACTACAGCCCCAAGTCT and reverse, TGGACCCATCTTCTATGC. We calculated the mitochondrial DNA copy number per cell by using Sdha amplification as a reference for nuclear DNA content.

**Western Blotting and Immunoprecipitation Assays.** Homogenates for Western blot analyses were obtained from either cell cultures or tissues. Cells were collected in ice-cold 1× PBS and homogenized with a douncer in lysis buffer [50 mM Tris (pH 7.5), 150 mM NaCl, 1% Triton X-100, 2 mM EDTA, 2 mM sodium orthovanadate, 50 mM NaF, 20 mM sodium pyrophosphate, and protease inhibitors mixture tablet (Roche)] and centrifuged at 700 × g for 10 min to remove nuclei, cell debris, and floating cells. Tissues samples were homogenized in 10 vol of lysis buffer with a Polytron. Homogenates were rotated for 1 h at 4 °C in an orbital shaker and centrifuged at 16,000 × g for 15 min at 4 °C. Proteins from total homogenates were resolved in 10% or 15% acrylamide gels for SDS/PAGE and transferred to Immobilon membranes (Millipore). The following antibodies were used: Mfn2, p-IRE1 and IRE1 (1/1,000; Abcam), p-Akt Ser<sup>473</sup>, phosphorylated insulin receptor substrate 1 (p-IRS1) Ser<sup>307</sup>, eukaryotic initiation factor 2α (eIF2α), p-eIF2α, binding immunoglobulin protein (BiP), p-p38 (Thr<sup>180</sup>/Tyr<sup>182</sup>), p38, pERK1/2 (Thr<sup>202</sup>/Tyr<sup>204</sup>), phosphorylated forkhead box protein O1 (pFOXO1) Ser<sup>256</sup>, and FOXO1 (1/1,000; Cell Signaling), IRS-1, p85 PI3K, and IRS2 (1/1,000; Upstate Biotechnology), IR-D and CCAAT/enhancer binding protein homologous protein (CHOP) (1/1,000; Santa Cruz), TORC2 and pTyr<sup>972</sup>-IR (1/1,000; Calbiochem), pTyr and ERK (1/1,000; BD), activating transcription factor 6 (ATF6) (1/1,000; Imgenex), β-actin (1/10,000; Sigma), α-tubulin (1/8000; Sigma), and porin (1/5,000; Calbiochem). The antibodies used for the detection of electron transport chain complexes were anti-NADH dehydrogenase (ubiquinone) 1α subcomplex 9 (NDUFA9; complex I), anti-SdhA (complex II), anti-ubiquinol-cytochrome *c* reductase core protein 2 (Uqcrc2; complex III), anti-COX IV (complex IV), and anti-Atp5a1 (complex V) (1/1,000; Molecular Probes). Proteins were detected by the ECL method (13) and quantified by scanning densitometry.

Immunoprecipitation of the insulin receptor and IRS-1 was performed in L6E9 myotubes, gastrocnemius muscle, and liver. Then, 1,000 μg of protein was immunoprecipitated with 5 μg/mL of either anti-IR-β or anti-IRS-1 antibody. Immunoprecipitates were collected on protein A Sepharose G beads, washed five times in lysis buffer, resuspended, and incubated for 5 min at 95 °C in Laemmli sample buffer, and subjected to SDS/PAGE.

**Enzymatic Activities.** The enzymatic activities of respiratory chain complexes and citrate synthase were measured spectrophotometrically in total lysates of tibialis muscles and liver. Activities of NADH:Q<sub>10</sub> oxidoreductase (complex I), succinate dehydrogenase (complex II), NADH:cytochrome *c* oxidoreductase (complex I, coenzyme Q and complex III: CI + III), succinatecytochrome *c* reductase (complex II, coenzyme Q and complex III: CII + III), decylubiquinol:cytochrome *c* oxidoreductase (complex III), cytochrome *c* oxidase (complex IV), and citrate synthase were determined following described spectrophotometric methods (14–16).

Muscle or livers homogenates were prepared by homogenizing frozen tissue in buffer and centrifuged according to the protocols

provided by the manufacturer. Total superoxide dismutase (SOD), catalase, glutathione reductase (GR), and glutathione peroxidase (GPx) activity were measured with commercial enzyme assay kits (Cayman Chemicals). Changes in absorbances were normalized by protein concentrations.

**Reduced Glutathione to Oxidized Glutathione (GSH/GSSG) Ratio.** GSH/GSSG ratio in liver and muscle samples was measured with a commercial kit (BIOXYTECH GSH/GSSG-412 assay kit; OxisResearch) as described previously (17, 18). Briefly, for GSSG measurement, tissue was homogenized in a solution containing 1 mM 1-methyl-2-vinylpyridinium trifluoromethanesulfonate to scavenge all reduced thiols in the sample. Total GSH and GSSG were then measured with the reagents and calibration set provided in the kit.

**Hepatocyte Isolation.** Collagenase perfusion was used to isolate hepatocytes from male control and liver-specific Mfn2 KO mice (25–28 g) as described in ref. 19. Cells were suspended in DMEM, supplemented with 10 mM glucose, 10% (vol/vol) FBS, 100 nM insulin (Sigma), and 100 nM dexamethasone (Sigma) and then seeded at a final density of 4 × 10<sup>6</sup> cells per cm<sup>2</sup> onto 60-mm-diameter plastic plates treated with 0.001% (wt/vol) collagen solution (Sigma). Media were replaced with fresh M99 media-free serum and 1% BSA and incubated for 12–14 h.

**Mitochondrial Morphology.** Mitochondrial morphology was analyzed with confocal microscopy (Leica Sp2) in live hepatocytes and longitudinal sections of skeletal muscle (tibialis anterior).

For transient transfection, hepatocytes cells were plated on coverslips and then transfected with Lipofectamine according to manufacturer's instructions. Then, 4 μg of pDsRed2-Mito vector (Clontech) was transfected for 24 h in M199 media, 1% BSA. Transfected cells were fixed in 4% paraformaldehyde, and mitochondrial morphology was analyzed with confocal microscopy.

For electroporated skeletal muscle (pDsRed2-Mito vector), tissues were fixed in 4% paraformaldehyde and subjected to a sucrose gradient from 10% to 30% in PBS. After that, muscles were included in O.C.T. solution (Sakura Tissue-Tek), and 10-μm cryosections were analyzed with a confocal fluorescence microscope. Images were processed with Image J software.

**ATP Extraction and Measurement.** Liver and muscle samples were immediately frozen in liquid nitrogen until the extraction procedure. The frozen tissue was powdered and homogenized in 0.5 mL of 0.6 M ice-cold HClO<sub>4</sub> and incubated for 10 min. The precipitated proteins were removed by centrifugation (10,000 × g for 10 min), and 300 μL of supernatant was neutralized by 1 M KHCO<sub>3</sub>. Ten microliters of supernatant was pipetted into the wells of a white nonphosphorescent microplate, placed in a luminometer (Luminoscan 1.2-0; Labsystems), and processed by addition of 90 μL of ATP monitoring reagent (ATP monitoring kit; Molecular Probes). ATP concentrations were calculated from a calibration curve constructed at the same time by means of standard ATP dissolved in the appropriate solution for each experiment.

**Statistical Analysis.** The data presented here were analyzed with the Student's *t* test or ANOVA with an appropriate post hoc test. Data are presented as mean ± SEM unless stated. Significance was established at *P* < 0.05.

- Chen H, McCaffery JM, Chan DC (2007) Mitochondrial fusion protects against neurodegeneration in the cerebellum. *Cell* 130:548–562.
- Heidt AB, Black BL (2005) Transgenic mice that express Cre recombinase under control of a skeletal muscle-specific promoter from *mef2c*. *Genesis* 42(1):28–32.

- Soriano FX, et al. (2006) Evidence for a mitochondrial regulatory pathway defined by peroxisome proliferator-activated receptor-γ coactivator-1α, estrogen-related receptor-α, and mitofusin 2. *Diabetes* 55:1783–1791.
- Liesa M, et al. (2008) Mitochondrial fusion is increased by the nuclear coactivator PGC-1β. *PLoS ONE* 3:e3613.

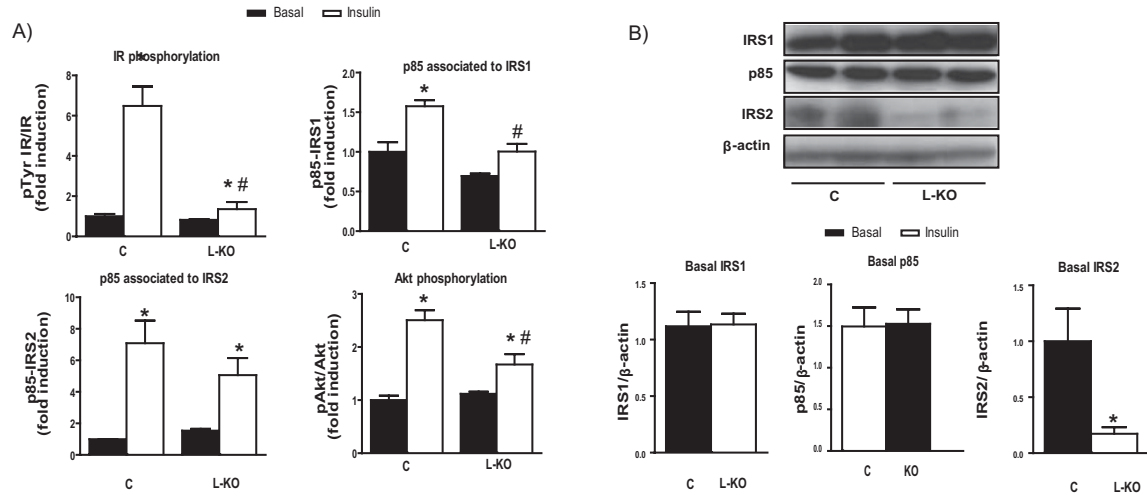
5. Perrin C, Knauf C, Burcelin R (2004) Intracerebroventricular infusion of glucose, insulin, and the adenosine monophosphate-activated kinase activator, 5-aminoimidazole-4-carboxamide-1- $\beta$ -D-ribofuranoside, controls muscle glycogen synthesis. *Endocrinology* 145:4025–4033.
6. Ozcan U, et al. (2006) Chemical chaperones reduce ER stress and restore glucose homeostasis in a mouse model of type 2 diabetes. *Science* 313:1137–1140.
7. Franckhauser S, et al. (2008) Overexpression of Il6 leads to hyperinsulinaemia, liver inflammation and reduced body weight in mice. *Diabetologia* 51:1306–1316.
8. McMahon JM, Signori E, Wells KE, Fazio VM, Wells DJ (2001) Optimisation of electrotransfer of plasmid into skeletal muscle by pretreatment with hyaluronidase—Increased expression with reduced muscle damage. *Gene Ther* 8:1264–1270.
9. Kaliman P, Viñals F, Testar X, Palacín M, Zorzano A (1996) Phosphatidylinositol 3-kinase inhibitors block differentiation of skeletal muscle cells. *J Biol Chem* 271:19146–19151.
10. Cantó C, et al. (2007) Neuregulins increase mitochondrial oxidative capacity and insulin sensitivity in skeletal muscle cells. *Diabetes* 56:2185–2193.
11. Kuznetsov AV, et al. (2008) Analysis of mitochondrial function in situ in permeabilized muscle fibers, tissues and cells. *Nat Protoc* 3:965–976.
12. Bach D, et al. (2005) Expression of Mfn2, the Charcot-Marie-Tooth neuropathy type 2A gene, in human skeletal muscle: Effects of type 2 diabetes, obesity, weight loss, and the regulatory role of tumor necrosis factor  $\alpha$  and interleukin-6. *Diabetes* 54:2685–2693.
13. Enrique-Tarancón G, et al. (2000) Substrates of semicarbazide-sensitive amine oxidase co-operate with vanadate to stimulate tyrosine phosphorylation of insulin-receptor-substrate proteins, phosphoinositide 3-kinase activity and GLUT4 translocation in adipose cells. *Biochem J* 350(1):171–180.
14. Birch-Machin MA, Briggs HL, Saborido AA, Bindoff LA, Turnbull DM (1994) An evaluation of the measurement of the activities of complexes I-IV in the respiratory chain of human skeletal muscle mitochondria. *Biochem Med Metab Biol* 51:35–42.
15. Fischer JC, et al. (1985) Differential investigation of the capacity of succinate oxidation in human skeletal muscle. *Clin Chim Acta* 153:23–36.
16. Rustin P, et al. (1994) Biochemical and molecular investigations in respiratory chain deficiencies. *Clin Chim Acta* 228(2):35–51.
17. Sinha-Hikim I, et al. (2011) A novel cystine based antioxidant attenuates oxidative stress and hepatic steatosis in diet-induced obese mice. *Exp Mol Pathol* 91:419–428.
18. Anderson EJ, et al. (2009) Mitochondrial H<sub>2</sub>O<sub>2</sub> emission and cellular redox state link excess fat intake to insulin resistance in both rodents and humans. *J Clin Invest* 119:573–581.
19. Massagué J, Guinovart JJ (1977) Insulin control of rat hepatocyte glycogen synthase and phosphorylase in the absence of glucose. *FEBS Lett* 82:317–320.







## Liver



## Skeletal muscle

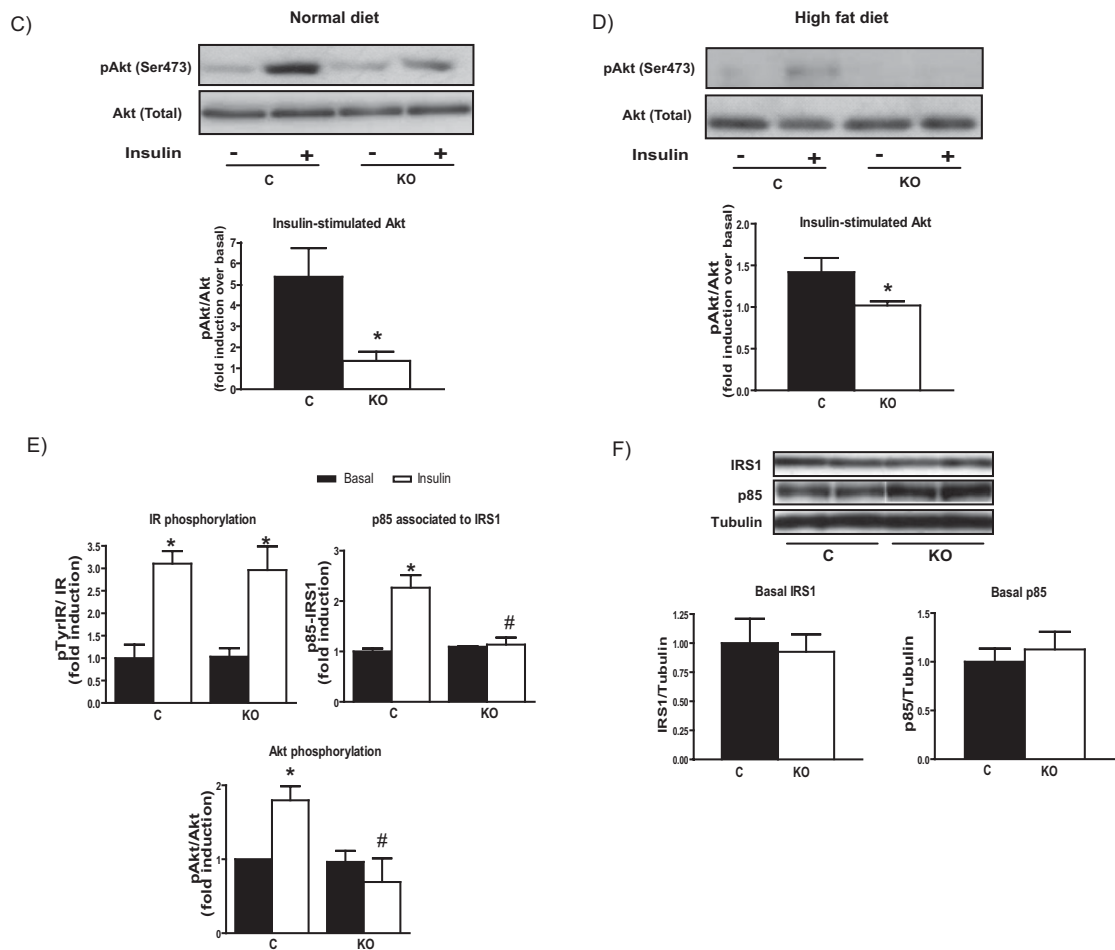


**Fig. S4.** (A) Quantification of insulin receptor (IR) tyrosine phosphorylation, p85 subunit of PI3K bound to IRS1 or IRS2, and Akt phosphorylation in liver extracts from C or L-KO mice on a normal diet 5 min after portal vein insulin injection ( $n = 6-8$  animals per group). (B) Total IRS1, IRS2, and p85 protein abundance analyzed in mice on normal chow-diet. A representative image and quantification of 6-8 animals per group are shown. (C) Akt phosphorylation was measured in soleus muscle from C and KO incubated with (30 nM) or without insulin for 15 min ( $n = 8$  mice per group). (D) Muscle response to insulin of mice on high-fat diet was evaluated by Akt phosphorylation in soleus muscle incubated with (100 nM) or without insulin for 15 min ( $n = 8$  mice per group). (E) Quantification of insulin receptor (IR) tyrosine phosphorylation, p85 subunit of PI3K bound to IRS1, and Akt phosphorylation in gastrocnemius extracts from C or KO mice on high-fat diet ( $n = 8-12$  animals per group). (F) Total IRS1 and p85 protein abundance analyzed in C or KO mice. A representative image and quantification of 6-8 animals per group are shown. Data represent mean  $\pm$  SEM. \* $P < 0.05$  vs. control group, and # $P < 0.05$  vs. insulin-stimulated control group.



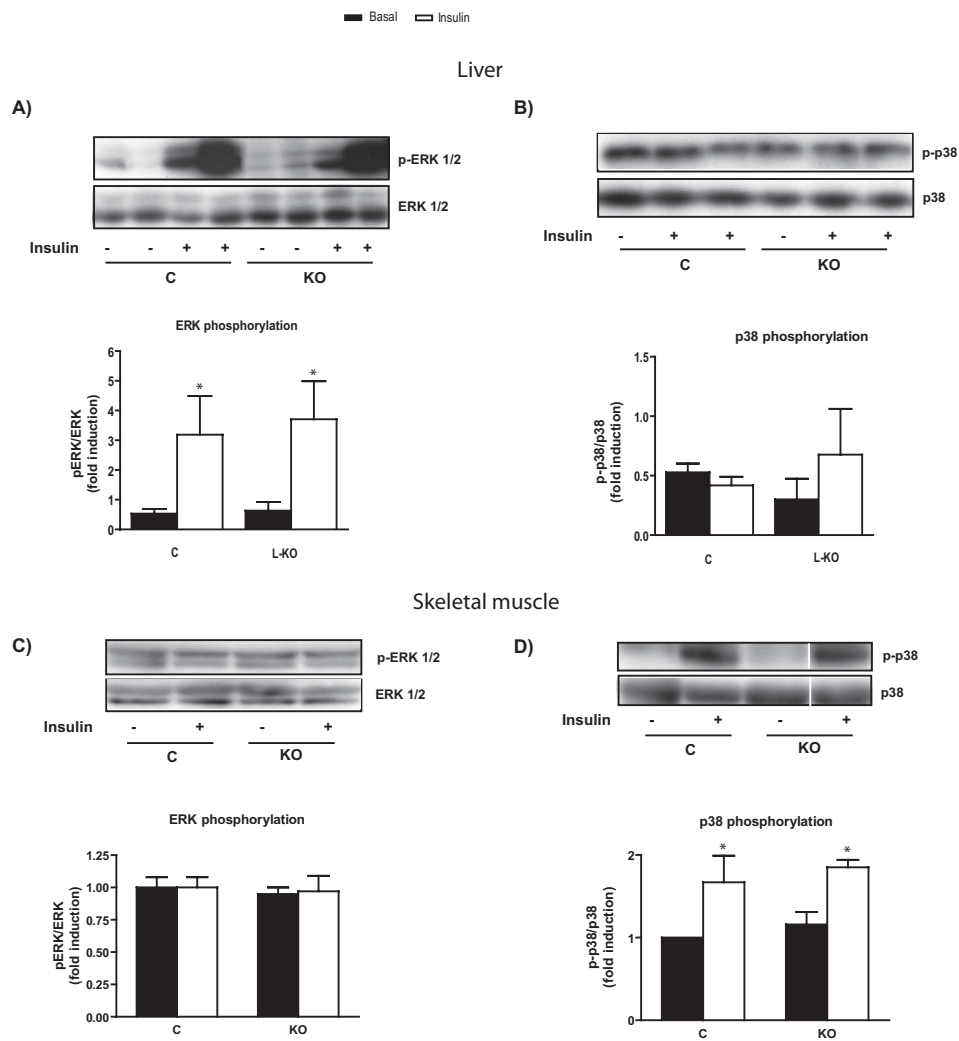


**Fig. S5.** ERK and p38 phosphorylation in liver-specific Mfn2 KO mice and Mfn2 KO mice. Insulin-stimulated ERK and p38 phosphorylation were evaluated by using specific antibodies in liver from L-KO mice and gastrocnemius muscle from Mfn2 KO mice subjected to a high-fat diet. Data represent mean  $\pm$  SE of the quantification of six animals per group. \* $P < 0.05$  vs. basal.

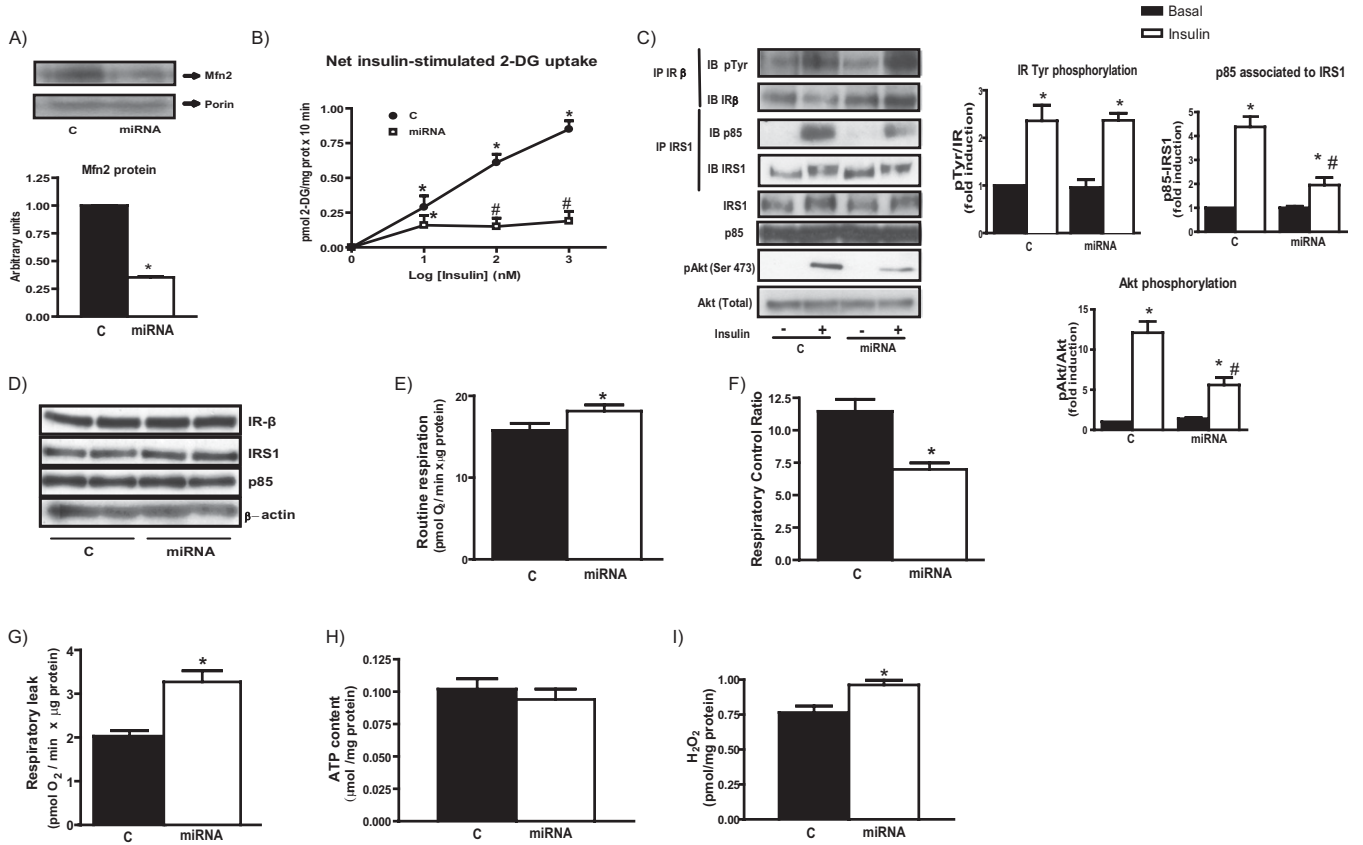


**Fig. 56.** Mfn2-silenced muscle cells show impaired insulin signaling and insulin action, mitochondrial dysfunction, and increased hydrogen peroxide levels. (A) Mfn2 protein levels in L6E9 myotubes transduced either with a control adenovirus (C) or an adenovirus encoding for a miRNA against Mfn2 (miRNA). Data were quantified by densitometry ( $n = 5$  independent experiments). (B) Uptake of 2-deoxyglucose was evaluated in control (C) and miRNA myotubes at a range of insulin concentrations (10, 100, and 1,000 nM) and represented as the net glucose uptake after insulin stimulation ( $n = 5$  independent experiments performed in duplicate). (C) Insulin signaling was evaluated in control (C) and miRNA L6E9 myotubes at 15 min after the addition of insulin (1  $\mu$ M). Insulin receptor (IR) tyrosine phosphorylation, p85 subunit of PI3K bound to IRS1, and Akt phosphorylation were measured with specific antibodies. A representative Western blot and the quantification of five independent experiments are shown. (D) Total protein expression levels of IR- $\beta$ , IRS1, and p85 were evaluated in control and miRNA L6E9 muscle cells. (E) Routine respiration (DMEM with 5.5 mM glucose) in C2C12 myotubes transduced with a control or a Mfn2 miRNA. (F) Respiratory control ratio in C2C12 myotubes. (G) Respiratory leak, measured after inhibition of ATP synthase with oligomycin, in C2C12 myotubes. (H) ATP content in control and miRNA muscle cells. (I) H<sub>2</sub>O<sub>2</sub> was measured in control and miRNA L6E9 muscle cells. Data represent mean  $\pm$  SEM. \* $P < 0.05$  vs. basal state or control group and # $P < 0.05$  vs. insulin-stimulated control group.

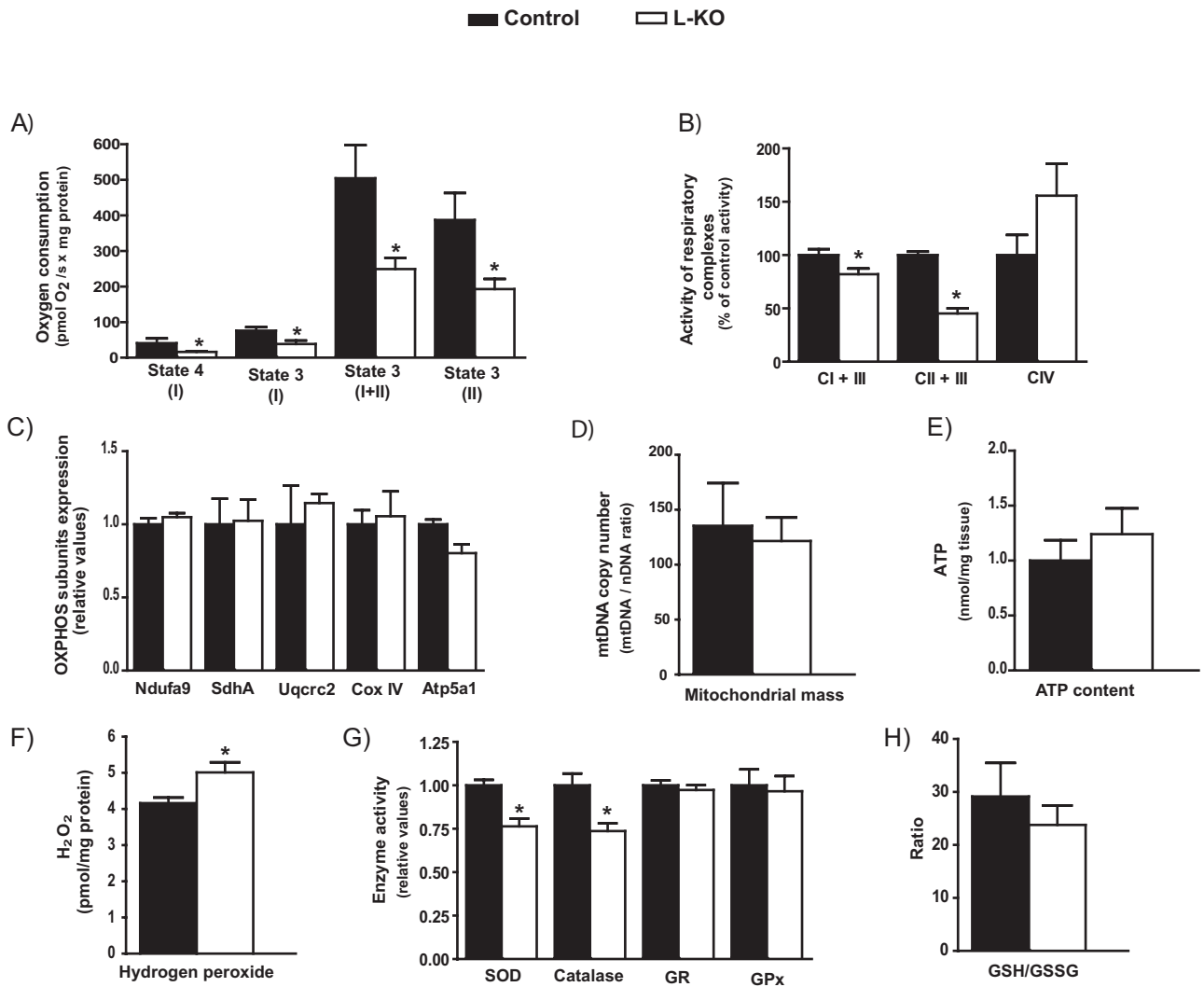


**Fig. S7.** Mfn2 ablation in liver leads to impaired mitochondrial respiration, impaired reactive oxygen species (ROS) handling, and increased concentration of hydrogen peroxide. (A) Mitochondrial respiration was assayed in isolated liver mitochondria (500  $\mu$ g) from control or L-KO mice ( $n = 5$  mice per group). (B) Respiratory complexes activities in liver. Data are given as a percentage of control values ( $n = 5$  mice per group). (C) Protein expression of subunits of respiratory chain complexes in liver. Data are expressed relative to  $\beta$ -actin. ( $n = 6$  per group). (D) Mitochondrial content assessed by mtDNA copy number in liver ( $n = 6$  per group). (E) ATP liver content ( $n = 5$  per group). (F) Hydrogen peroxide was measured in liver from control and L-KO mice ( $n = 8-10$  mice per group). (G) Activity of SOD, catalase, GPx, and GR was assayed in liver from control and L-KO mice. Activity is expressed as relative values compared with control mice ( $n = 8$  mice per group). (H) GSH/GSSG ratio was determined in liver from control and L-KO mice ( $n = 8$  mice per group). Data represent mean  $\pm$  SEM. \* $P < 0.05$  vs. control mice.

■ Control    □ Mfn2 deficiency

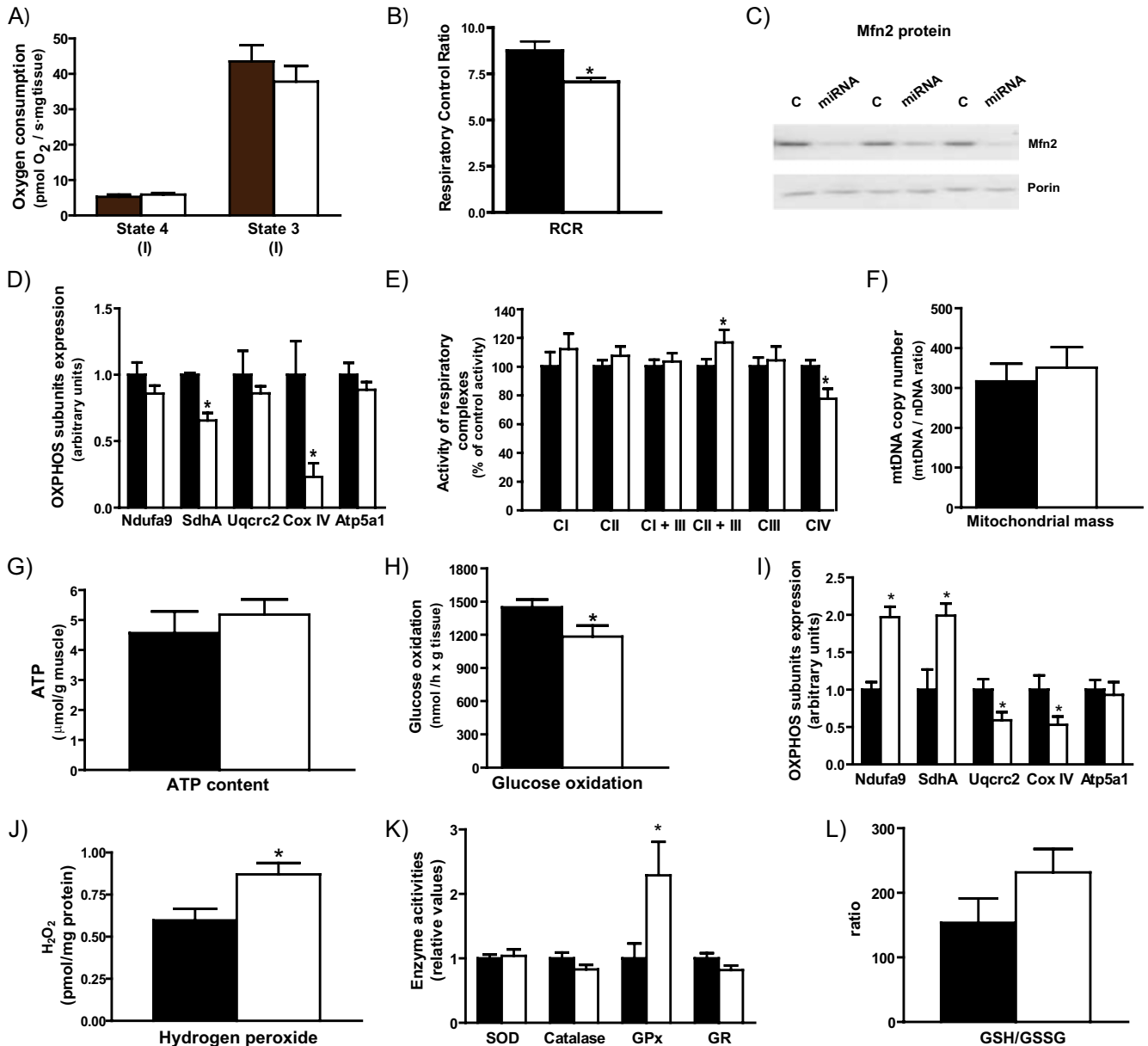


**Fig. 58.** Mfn2 loss of function in skeletal muscle leads to an impaired mitochondrial respiration and increased concentration of ROS. (A) State 3 and state 4 respiration was assayed in permeabilized fibers from tibialis muscle from control or KO mice, with complex I substrates ( $n = 6$  mice per group). (B) Respiratory control ratio (RCR) (state 3/state 4) in permeabilized muscle fibers. (C) Mfn2 and porin protein levels in gastrocnemius electrotransferred with a control or a Mfn2 miRNA. (D) Protein expression of subunits of respiratory chain complexes in mitochondrial fraction of gastrocnemius electrotransferred with a control or Mfn2 miRNA. Data are expressed relative to porin ( $n = 6$  per group). (E) Respiratory complexes activities in muscle from mice electrotransferred with a control or a Mfn2 miRNA. Data are given as a percentage of control activity ( $n = 10-12$  mice in each group). (F) Mitochondrial content assessed by mtDNA copy number in gastrocnemius muscle ( $n = 6$  per group). (G) ATP content in gastrocnemius from control and Mfn2 KO mice ( $n = 8$  mice per group). (H) Glucose oxidation assays were performed in soleus muscle from control or KO mice ( $n = 9-12$  observations per group). (I) Protein expression of subunits of respiratory chain complexes in mitochondrial fraction of soleus from control and Mfn2 KO mice. Data are expressed relative to porin ( $n = 7$  mice per group). (J) H<sub>2</sub>O<sub>2</sub> was measured muscle from control or KO mice ( $n = 8-10$  mice per group). (K) Activity of SOD, catalase, GPx, and GR was assayed in gastrocnemius muscle from control and Mfn2 KO mice. Activity is expressed as relative values compared with control mice ( $n = 8$  mice per group). (L) GSH/GSSG ratio was determined in gastrocnemius muscle from control and KO mice ( $n = 8$  mice per group). Data represent mean  $\pm$  SEM. \* $P < 0.05$  vs. control mice.

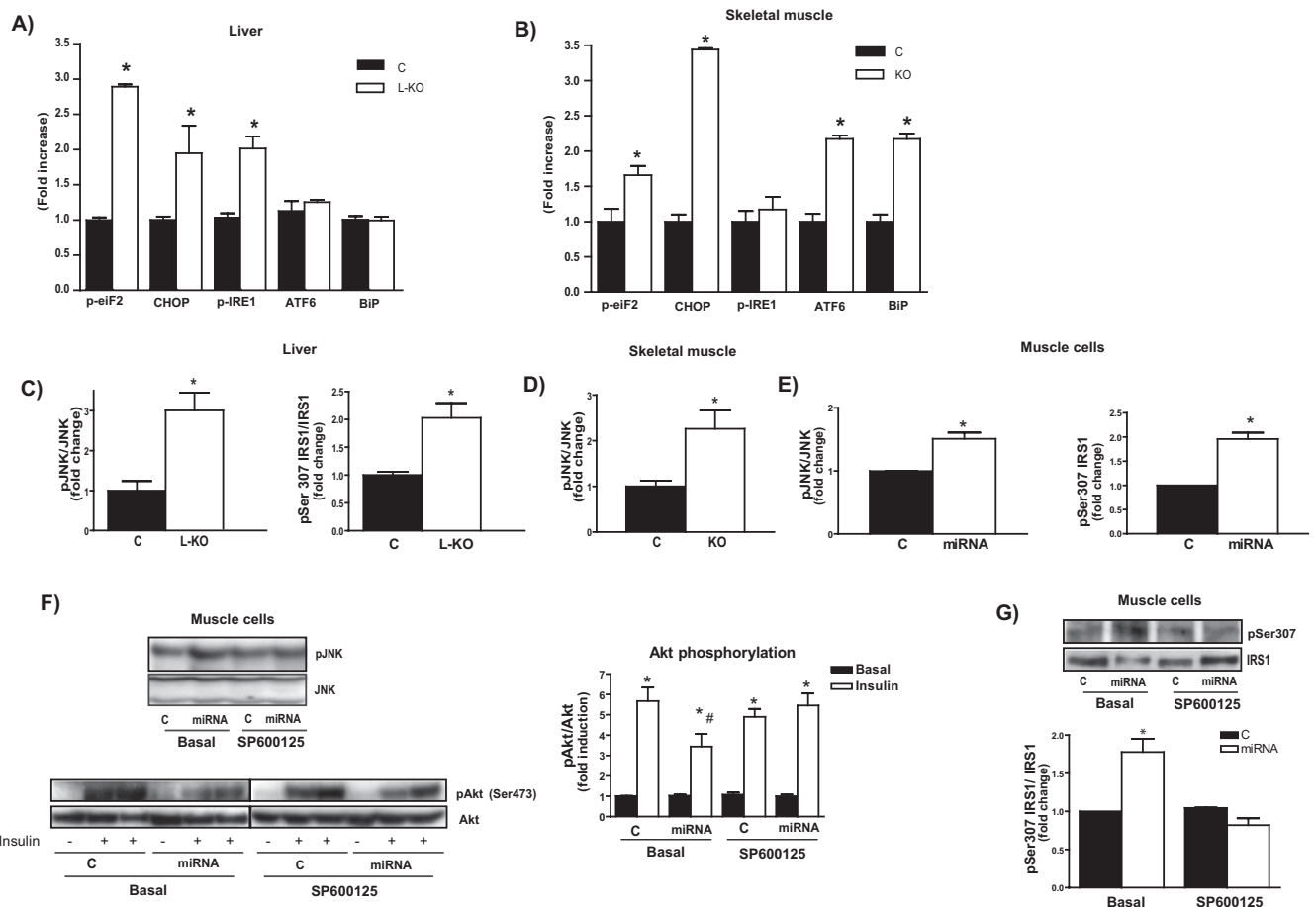


**Fig. S9.** Mfn2 ablation causes ER stress and JNK activation. (A and B) Quantification of ER stress markers in liver from C and L-KO mice (A) and in skeletal muscle from C and KO mice (B) ( $n = 6-8$  animals per tissue and group). (C-E) Quantification of pJNK in liver of C and L-KO mice (C), skeletal muscle from C and KO mice (D), and L6E9 myotubes (E) ( $n = 5$ ). Quantification of Ser 307 phosphorylation of IRS1 in livers from C and L-KO mice (C) and L6E9 myotubes (E) ( $n = 5$ ). (F) JNK phosphorylation and insulin-stimulated Akt phosphorylation ( $1 \mu\text{M}$  insulin for 15 min) in control and Mfn2 miRNA transduced L6E9 myotubes treated with or without the JNK inhibitor SP600125 at  $10 \mu\text{M}$  ( $n = 3$  independent experiments performed in duplicate). (G) Western blot analysis of IRS1 Ser307 phosphorylation in the absence or presence of SP600125 ( $10 \mu\text{M}$ ) in control or Mfn2 miRNA transduced L6E9 myotubes ( $n = 3$  independent experiments). \* $P < 0.05$  vs. no insulin and # $P < 0.05$  vs. insulin-stimulated control group (in F and H).

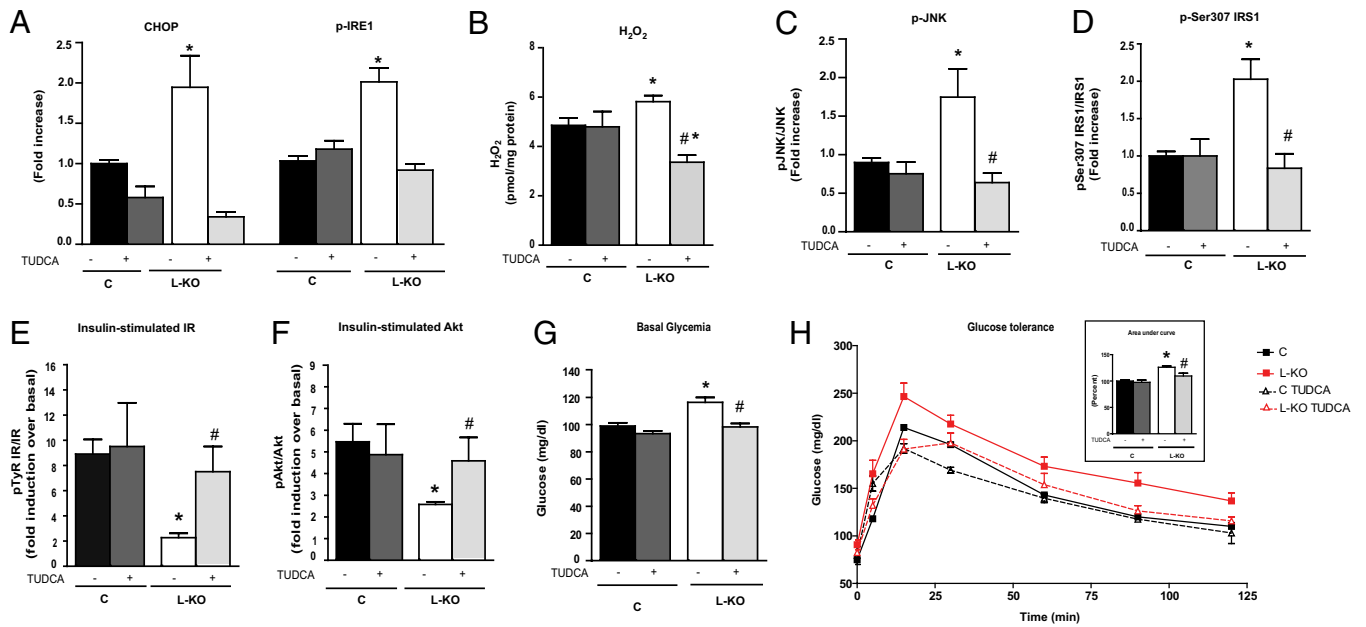


**Fig. S10.** Mfn2 deficiency causes ER stress, and TUDCA treatment reverses insulin resistance. Data are shown for control and L-KO mice before and after TUDCA treatment. (A) Quantification of ER stress markers. (B) Hydrogen peroxide content. (C) JNK phosphorylation. (D) Fold increase of Ser<sup>307</sup> phosphorylation of IRS1. (E and F) Fold increase of insulin receptor phosphorylation (E) or Akt serine phosphorylation (F) after insulin stimulation. (G) Basal glycemia. (H) GTT assays (area under the curve shown in *Inset*). Data represent mean ± SEM (*n* = 8–10). \**P* < 0.05 vs. control group and #*P* < 0.05 vs. untreated L-KO group.

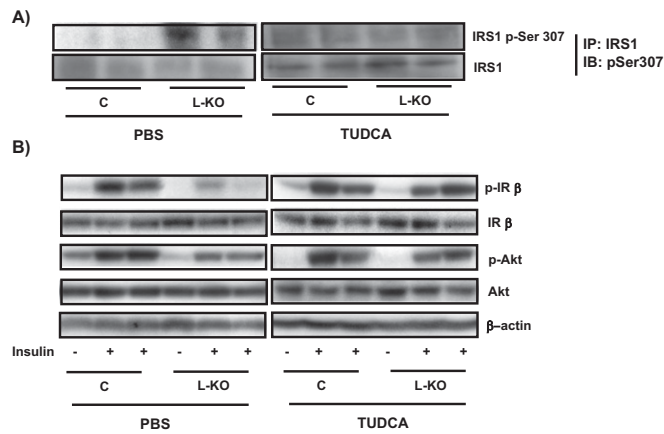


**Fig. S11.** Effects of treatment with TUDCA on insulin signaling in L-KO mice. Control and L-KO mice before and after TUDCA treatment. Representative Western blots are shown for insulin-stimulated IRS1, insulin receptor phosphorylation, and Akt serine phosphorylation.

